

Effects of Icing on Performance of a Research Airplane

William A. Cooper,* Wayne R. Sand,† Marcia K. Politovich,‡ and Donald L. Veal§
University of Wyoming, Laramie, Wyoming

The difference between the normal and actual rates of climb of a research airplane is used to measure the effect of icing on performance. The icing conditions were encountered in the course of an extensive series of meteorological research flights in various locations and seasons. Coefficients of lift and drag were determined for the airplane before and after icing encounters, and those coefficients were used to predict airplane performance for various flight conditions. The effect of icing was to increase the drag significantly, while there was little effect on the coefficient of lift. In the course of these flights, characteristics of the icing clouds (such as hydrometeor size spectrum and phase, liquid water content, temperature, etc.) were also measured, and those characteristics are compared to the summaries in the Federal Aviation Regulations and to the data sources on which those summaries were based. Most measurements lie within the envelopes suggested by earlier studies. For volume median diameters larger than $30\mu\text{m}$, the liquid water contents were substantially lower than indicated by those summaries, but for other diameters measured liquid water contents extended up to and, in rare cases, exceeded the limiting envelopes of the Regulations. Two exceptional cases of icing associated with droplets of 40 – $300\mu\text{m}$ diameter are also discussed. The reduction in performance during these cases was anomalously large, although the liquid water content and volume median diameter did not indicate that these cases should have been potentially hazardous.

Introduction

TO acquire the measurements needed for meteorological research, instrumented aircraft often must fly in icing conditions. In this paper, the icing encountered by one such research airplane, the Wyoming Super King Air (N2UW), is examined. The microphysical characteristics of the icing clouds were measured while the performance of the airplane was monitored. The observed changes in performance provide a measure of the severity of different icing environments.

Some characteristics of the icing encounters were discussed by Sand et al.¹ Summaries of the liquid water contents, median volume diameters, and other characteristics of the clouds that caused airframe icing were presented, and some effects of ice accretion on performance were also discussed. In this paper, we extend those considerations in two ways. First, a direct comparison to the characterization of icing in the Federal Aviation Regulations² (Part 25, Appendix C), and to the reports on which that Appendix was based, is presented. Second, the effects of icing on the lift and drag of this airframe are studied, and the extent to which the icing hazard is characterized by summaries such as those of Appendix C is considered.

Characteristics of the Research Airplane

The airplane used was a Beechcraft Super King Air Model 200T (Fig. 1) with reinforced outer wing panels to accommodate wing tip mounting of sensors and probes. This airplane, which has a heated propeller and pneumatic boots on the wings and horizontal stabilizer, is certified for flight into known icing conditions.

Several modifications were made to the basic 200T airframe. Wing tip pylons were added on which instruments were mounted to measure microphysical properties of clouds,

and a 2 m decelerator was mounted above the fuselage for the collection of samples of ice crystals. In addition, the airplane was modified by the addition of a Saunders Failsafe spar strap, which consists of a stainless steel strap extending from the inboard segment of the outer wing panels through the wheel well and under the airplane. The protrusion below the wing is minimal outboard of the engine nacelles. However, below the center section, the fairing extends downward about 2.5 in.

The data acquisition on this airplane is controlled by a microprocessor linked to an onboard computer. The computer converts the data to scientific units for display in the airplane, while the microprocessor controls data recording on computer compatible magnetic tape. Table 1 lists the instrumentation on the airplane during these studies. The following paragraphs discuss some measurements of particular importance to this paper.

Cloud Droplet Sizes and Concentrations

The primary instrument for the detection of cloud droplets was a Forward Scattering Spectrometer Probe (FSSP), manufactured by Particle Measuring Systems (PMS), Inc. This probe sizes and counts individual cloud droplets by detecting the light scattered from the laser beam as the droplets pass through its aperture. The detected pulses are converted to droplet size by a pulse height analyzer so that the instrument provides a continuous measurement of the complete cloud droplet size distribution. Independent measurements of the droplet spectrum were made each 0.1 s (or approximately each 10 m of flight). Our instrument has undergone extensive testing and intercomparison with other devices (e.g., see Ref. 3) and has been calibrated by use of glass beads and Mie scattering calculations.⁴

Liquid Water Content

The liquid water content was calculated from the droplet spectrum measured by the FSSP. In addition, a standard Johnson Williams (JW) hot wire device⁵ for the measurement of liquid water content was operated. During recent studies (since 1981), measurements from a CSIRO liquid water sensor⁶ and a Rosemount icing probe were also recorded.

Received March 10, 1984. Copyright © American Institute of Aeronautics and Astronautics, Inc. 1984. All rights reserved.

*Associate Professor, Department of Atmospheric Science.

†Assistant Professor and Flight Facility Manager, Department of Atmospheric Science, Member AIAA.

‡Graduate Student, Department of Atmospheric Science.

§President.

The JW probe has been calibrated and intercompared with many other probes in the Ottawa wind tunnel of the National Research Council of Canada.⁷ A sample of the calibrations was shown by Sand et al.¹ Other evidence for the accuracy of the measurements was presented by Boatman,⁸ who compared measurements of liquid water content with theoretical values in unmixed cores of vigorous clouds.

The liquid water contents measured by the JW probe and the FSSP were compared for a one-month period, with the result that the best fit to the simultaneous measurements was $LWC(JW) = 0.96 \times LWC(FSSP) + 0.01 \text{ g/m}^3$. Results from the two probes were thus in good agreement. Periods when there were significant disagreements between these two probes have been excluded from this study.

Ice Particles and Rain Drops

The four PMS probes listed in Table 1 provided complete information regarding the sizes and concentrations of ice crystals and raindrops. In addition, the two dimensional probes recorded two dimensional images of the particles passing through their sampling apertures, so that ice particles could be distinguished from water drops on the basis of shape.

Performance Monitoring

The torque delivered by the left engine was measured and recorded to permit monitoring of airplane performance. Additional measurements related to performance included the ground speed and drift angle (determined by a Doppler radar until 1982, and since then by an inertial navigation system);

the indicated airspeed; angle of attack; yaw, pitch, and roll angles; and vertical and (since 1982) horizontal acceleration.

State Parameters

The primary temperature sensor was designed to remain dry during flight through clouds.⁹ It was supplemented by another temperature sensor, Rosemount Model 102; although not similarly protected against wetting, it was deiced. The dew point, pressure, airplane position and altitude, and other parameters listed in Table 1 were also recorded.

Comparison to FAR, Part 25, Appendix C

The data sources used for these studies are listed in Table 2. All cloud regions colder than 0°C where the instruments worked reliably have been included. General characteristics of



Fig 1 Research airplane N2UW as modified with wing tip pylons, decelerator (tube on top), and noseboom.

Table 1 Instrumentation on the research airplane

Measurement	Instrument	Manufacturer	Response	Accuracy	Resolution
Temperature #1	Platinum resistance	Rosemount Model 102	<1 s	±0.5°C	<0.1°C
Temperature #2 (reverse flow)	Platinum	NCAR design Minco element	<0.5 s	±0.5°C	<0.1°C
Dew point	Cooled mirror	Cambridge Model 137C3	3°C/s (slew rate)	±0.5°C (>0°C) ±1.0°C (<0°C)	0.3°C
Heading ^a	Magnetic	King KP1 553	1 s	±1 deg	0.1 deg
Altitude	Pressure	Rosemount 1201FA1B1A	15 ms	±4 mb	0.3 mb
Altitude	Radar altimeter	Stewart Warner APN 159	152 m/s (slew rate)	2.4 m or 1%	0.07 m
IAS	Differential pressure	Rosemount 831 CPX	25 ms	±1 mb	0.1 mb
Rate of climb ^a	Differential altitude	Rosemount 1241 A 4BCDE	50 ms	1% to 4.5 km 2% to 8 km	0.25 m/s
Position	VOR	King KNR 615	1 s	1.5 deg	
	DME	King KDM 705A	1 s	0.4 km	0.2 km
	INS	Litton LTN51			
Vertical acceleration ^a	Stabilized accelerometer	Humphrey SA-09 0502 1	10 μs	0.002 g	
Pitch/roll ^a	Stabilized accelerometer	Humphrey SA 09 0502 1	10 μs	0.2 deg	
Ground speed ^a	Doppler radar	Singer	1 s	0.17% ± 2 m/s	0.5 knot
Drift angle ^a	Doppler radar	Singer	2 s	0.2 deg	0.2 deg
Yaw/attack angles	Differential pressure	Rosemount 858AJ28	0.1 s	0.2 deg	<0.1 deg
Turbulence	Pressure	M R I	3 s	10%	1%
Liquid water content ^b	Hot wire (JW)	Bacharach Instruments Model LWH	<1 s	0.2 g/m ³	0.1 g/m ³
Liquid water content	CSIRO hot wire	University of Wyoming	~10 ms	0.1 g/m ³	0.05 g/m ³
Liquid water content	Icing probe	Rosemount	>5 s		
Droplet size	FSSP	PMS	0.1 s	2 μm	2 μm
Hydrometeor size and shape	IDC	PMS	0.1 s	12.5 μm	12.5 μm
	2DC	PMS	μs	25 μm	
	2DP	PMS	μs	200 μm	

^a Also measured by the inertial navigation system (INS) since 1981. ^b Also measured by the FSSP.

Table 2 Sources of data

Date	Area	Flight hours
Winter 1978	California	104
Winter 1979	California	116
Winter 1980	California	99
Winter 1982	California	8
Summer 1978	Montana	91
Summer 1979	Montana	156
Summer 1980	Montana	140
Summer 1981	Montana	170
Winter 1978	Utah	35
Summer 1978	Florida	35
Spring 1978	Kansas	38
Summer 1980	Illinois	24
Winter 1981	Michigan	45
Winter 1981	Great Plains	30
Total		1091

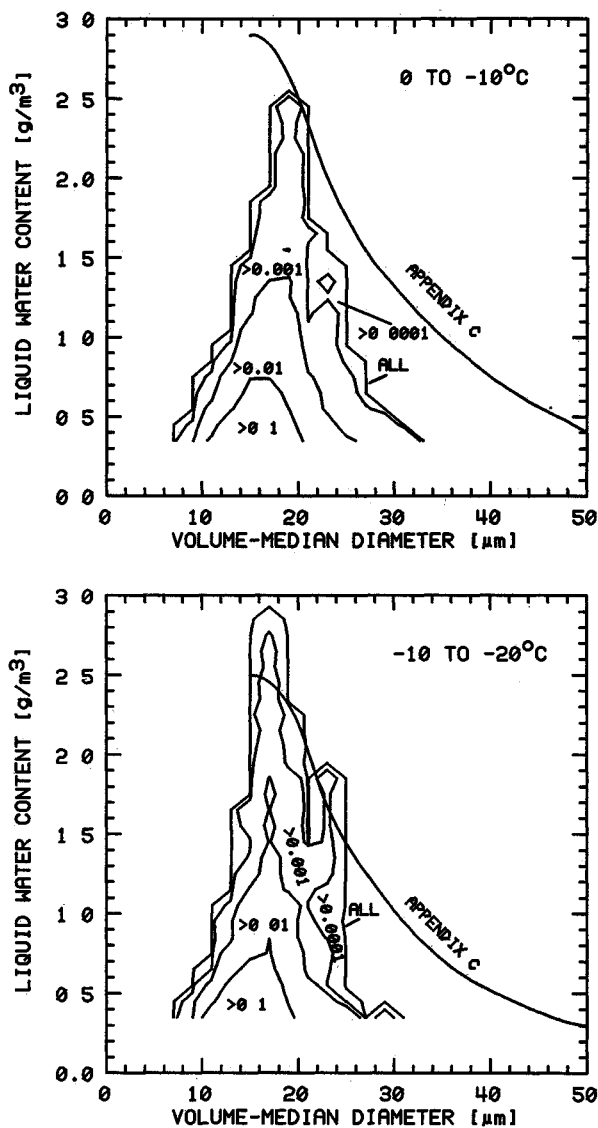


Fig 2 Comparison between the observations of this study and the envelope of FAR, Part 25, Appendix C, for the intermittent maximum distance of 2.6 n mi. The outside contour (labeled 'all') encompasses all observations, and the other contours indicate probability densities in units of $(\mu\text{m g/m}^3)^{-1}$. There were 46,992 measurements used to construct the top plot (for 0 to -10°C), and 21,149 measurements used for the bottom plot (for -10 to -20°C), all having 2.6 n.mi. average liquid water contents greater than 0.3 g/m^3 .

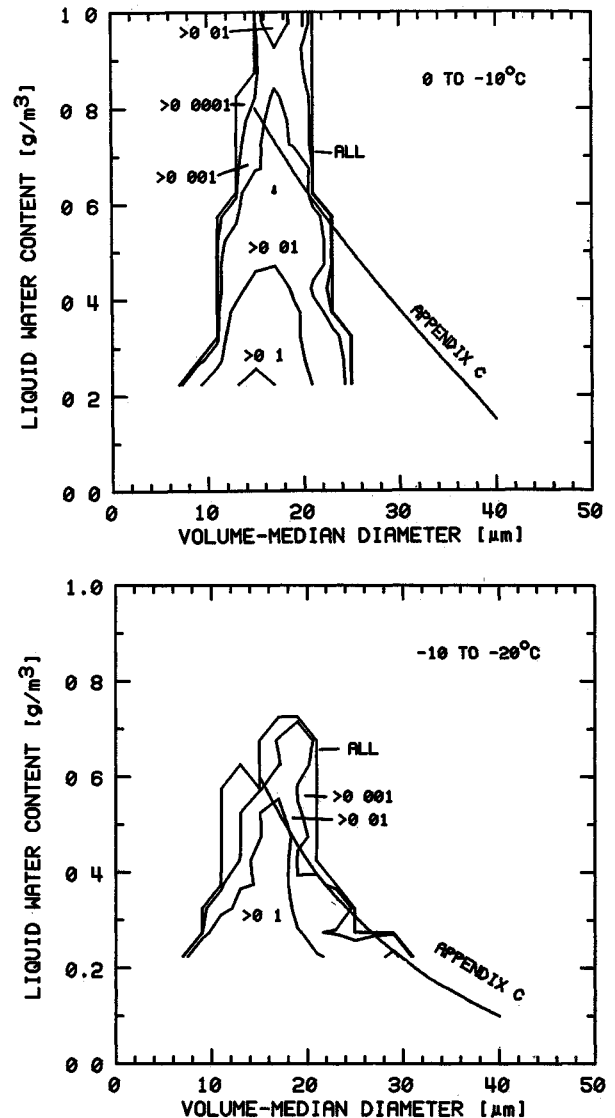


Fig 3 Comparison between the observations of this study and the envelope of FAR, Part 25, Appendix C, for the continuous maximum distance of 17.4 n mi. The outside contours indicate probability densities in units of $(\mu\text{m g/m}^3)^{-1}$. There were 52,777 measurements used to construct the top plot (for 0 to -10°C), and 20,999 measurements used for the bottom plot (for -10 to -20°C), all having 17.4 n mi average liquid water contents greater than 0.2 g/m^3 .

the icing encounters can be found in Sand et al.¹ Herein we specifically compare the measurements to the summaries in the Federal Aviation Regulations.

The FAA requirements for certification for flight into known icing conditions are based on FAR, Part 25,² Appendix C (hereafter referred to as Appendix C). Appendix C defines two icing categories: continuous and intermittent. The "maximum continuous" icing condition is the extreme expected for an icing encounter lasting 17.4 n mi (32.2 km), while the "intermittent maximum" condition is the extreme expected for 2.6 n mi (4.8 km). Interpolation factors are given for use with distances other than these standard distances. The nature of the icing encounters is characterized by two parameters: the average liquid water content (LWC) and the volume median diameter (D_v). D_v is defined so that half of the liquid water content is contained in droplets larger than and half in droplets smaller than D_v .

For comparison to Appendix C, the measurements of LWC and D_v from the flights listed in Table 2 have been averaged over distances of 2.6 and 17.4 n mi. and then have been plotted in the format of Appendix C. Values of LWC and D_v

were measured once each second (or about once each 100 m of flight) so that, for example, the 2.6 n.mi. averages were obtained from sets of approximately 48 1 s measurements. Each 48-s interval was used to represent one average value, with the intervals allowed to overlap.

The flights generally were conducted to study precipitation formation processes and, hence, emphasized regions with high liquid water content. The probabilities characterizing these flights are overestimates of the probabilities of similar icing encounters during routine flight operations. Regions of high liquid water content were often penetrated repeatedly, further increasing the exposure to icing conditions.

The respective data for the intermittent maximum and the continuous maximum distances are shown in Figs. 2 and 3. Data from all temperatures less than 0°C have been combined, and herein are compared to the <0°C (or most inclusive) limit of Appendix C.

The intermittent-maximum icing envelopes of Appendix C encompass our data well for drop sizes smaller than about 25 μm . The envelopes could be reduced to about 70% of the indicated liquid water contents, and only about 1% of the measurements would lie outside them. The continuous maximum envelopes were exceeded in about 1% of the icing encounters, but the authors attribute this primarily to the flight patterns which frequently returned to regions where the icing was the greatest.

The primary discrepancy between the authors' observations and the envelopes of Appendix C is that no values of $D_v > 30 \mu\text{m}$ were found associated with liquid water contents greater than 0.2 g/m³, although the envelopes of Appendix C encompass considerably higher liquid water contents for D_v from 30–50 μm . The FSSP, the primary instrument used to determine these sizes, measured diameters up to 45 μm when appropriate, and those measurements have been supplemented by measurements that cover the entire hydrometeor size spectrum.

To study this discrepancy we have examined some other sources. Lewis et al.,^{10,11} the primary sources of data for the charts in Appendix C, show only four observations with D_v exceeding 40 μm . None of the four observations exceeds the liquid water threshold used for the plots presented herein (0.2 g/m³ for continuous icing and 0.3 g/m³ for intermittent icing). Jeck¹² also found no values of D_v larger than 35 μm .

and no values larger than 30 μm in regions where the liquid water content exceeded 0.2 g/m³. Thus, we have not found data to support the extension of the envelopes to drop diameters exceeding 35 μm .

With this major exception these new observations generally support the envelopes of Appendix C. This is a useful result for two reasons. First, the data used by Jones and Lewis,¹³ on which Appendix C is based, were collected primarily in the wintertime in the northern United States. It was an admitted weakness in the data set that icing in other parts of the country or in other seasons was not represented. The inclusion of observations from the Great Plains, Florida, and California is thus a useful addition. Second, the data presented herein come from a new generation of cloud physics instrumentation, which provides high resolution measurements. In particular, the droplet size spectrum is measured in 15 size intervals spanning sizes from 1.45 μm , and additional measurements span the entire hydrometer size range. These instruments provide a very complete characterization of the microphysical properties of the icing clouds and make the analysis of large data sets possible.

Effects of Ice on Performance

Theory

The accretion of ice on an airframe affects performance primarily through induced aerodynamic changes and through effects on the powerplant. The latter will not be considered in this report; torque delivered by the left engine was measured and recorded, and these records verify that there has been no reduction in power which could be attributed to the effects of icing. The weight of the accreted ice seldom amounts to more than a few percent of the airplane weight, so that effect will also be ignored in the following discussion. Another possible effect of icing is to reduce the efficiency of the propellers, but since the propellers on this airplane are deiced and normally stay clean, we have used the propeller efficiencies quoted by the manufacturer.

The predominant effects of icing can then be described by the effects on the lift and drag of the airframe. The development followed herein is to determine coefficients of lift (C_L) and drag (C_D) for the clean airframe and for the airframe after icing has occurred. In addition to separating the effects on lift and drag, this procedure has the advantage that once C_L and C_D are known the performance of the airplane can be calculated for various power settings, air speeds, and air densities. Thus, a short set of flight maneuvers, sufficient to determine C_L and C_D , permits prediction of the performance of the airplane for a wide range of possible flight conditions.

The horizontal and vertical equations of motion form the basis for the calculations. The approach was similar to that of Lenschow.¹⁴ Measurements of angle of attack, pitch, indicated and true airspeed, and vertical and horizontal acceleration were used, along with the measured torque from the engines, the known propeller rotation rate, and the propeller efficiencies quoted by the manufacturer. From these measurements, the effective coefficients of lift and drag were found; these were used with the wing area of 28 m², although lift and drag actually result from the effects of the entire airframe.

C_L was determined as a function of angle of attack, and C_D as a function of C_L^2 . Prior to the installation of the inertial navigation system in 1982, the horizontal acceleration needed to determine C_D had to be determined from differentiating ground speed measured by a Doppler radar. Because of poor resolution in that procedure, fits to the data yielded inaccurate functional dependences of C_D , therefore only mean values of C_D (without dependence on C_L) have been determined for cases before 1982. This still provides useful results because induced drag, normally the source of strong dependence on C_L , is not included in the drag coefficient as

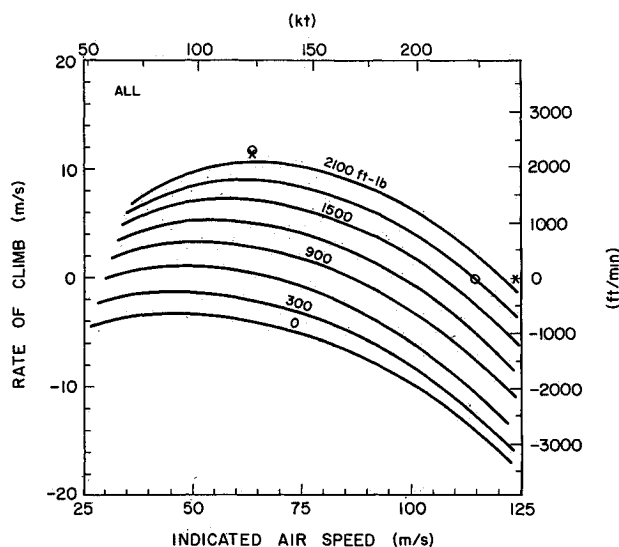


Fig. 4 Rate of climb as a function of airspeed and power setting for a clean airframe weighing 12,000 lb and an air density 80% of standard. Parameters on the curves represent engine torque (per engine) in ft-lb. The points marked "o" are taken from the pilot manuals for the Beechcraft 200T, while nearby points marked "x" are corresponding points from the calculations. A propeller rotation rate of 1700 rpm was assumed.

formulated by Lenschow, but rather is explicitly included in the equations of motion as a separate term dependent upon lift

Once C_L and C_D were determined the predicted rate of climb of the airplane was determined as a function of indicated airspeed and power setting. For unaccelerated flight, the horizontal and vertical equations of motion specify two relationships among the four variables thrust, angle of attack (α), pitch (θ), and indicated airspeed. For specified thrust and indicated airspeed, the rate of climb in still air can be found from $w = V(\alpha - \theta)$, where w is the rate of climb and V is the true airspeed. The effects of altitude and temperature are incorporated when thrust is obtained from torque and when true airspeed is obtained from indicated airspeed.

Application to the Clean Airframe

The coefficients of lift and drag were determined for the clean airframe by use of special maneuvers which covered a range of angles of attack and airspeeds. Since this airplane has been modified from the standard 200T configuration by the addition of pylons and instruments, it was important to determine these values experimentally rather than to rely upon those quoted by the manufacturer. Also, the ability to calculate realistic performance values serves as a check on the procedures.

An inertial navigation system was used to provide accurate measurements of accelerations and orientation angles. Several sets of maneuvers were used. Porpoising maneuvers involved varying pitch angle with repeated climbs and descents at constant power settings. A set of acceleration deceleration maneuvers with no altitude change was also flown to isolate the effects of the coefficient of drag.

The coefficients determined by a least squares fit to data from the combined maneuvers were: $C_L = 0.220 + 6.16\alpha$ and $C_D = 0.024 + 0.033C_L^2$. Individual flight segments yielded coefficients that varied by about $\pm 5\%$ from these.

Figure 4 shows the performance deduced from the combination of all maneuvers. For comparison two points selected from the Beechcraft manuals are also shown. The maximum climb rate is close to that obtained from these coefficients of lift, although the maximum speed for level flight is somewhat less than predicted. The discrepancy at

high airspeed may be the result of increased drag due to the modifications to the airplane, or it may reflect poor extrapolation far from the 70-100 m/s airspeed range in which we normally operate and in which these tests were conducted. The predicted rates of climb deduced from the different sets of porpoising maneuvers varied by about 1 m/s (rms deviation) in the 60-100 m/s range, so flight maneuvers of about 3 min duration can be used to predict rates of climb with this precision.

As a check on the accuracy of the predictions, a comparison was made of the predicted rates of climb with actual rates of climb at the start of all flights. Only those periods of the flights before any icing was encountered were considered. The rms error in the prediction¹ was 1.2 m/s, even though there were some variations in weight of the airplane that were not taken into account. Thus, the predicted rates of climb for the clean airplane have an overall accuracy of about 1.2 m/s.

Effects of Typical Icing Encounters

Sand et al.¹ showed that, for this airplane with ice protection equipment in use, the path integral of the supercooled liquid water content (termed the potential accumulation) correlated well with the effects on performance. The rate of climb decreased by about 1.8 m/s for any accumulation (partly attributable to the ice protection systems, including ice vanes) and decreased an additional 0.45 m/s for each additional g/cm² of potential accumulation. The effect on performance showed no correlation with D_v .

Since a potential accumulation of 1 g/cm² corresponds to flight through a 10 km region of 1 g/m³ liquid water content, these results indicate that this airplane can fly with ease in the icing conditions described in Appendix C. For example, in the extreme intermittent maximum liquid water content (3 g/m³ over a distance of 2.6 n mi), the corresponding reduction in climb ability is only about 2.5 m/s. For the extreme continuous maximum condition (0.8 g/m³ over 17.4 n mi) the corresponding reduction is about 3 m/s. Since this airplane can climb at 5.10 m/s under the typical conditions where ice is encountered, there is ample reserve performance to handle such icing encounters.

An example of the performance of the airplane after an icing encounter is shown in Fig. 5. On March 3, 1980, icing conditions were encountered upwind of the Sierra Nevada Mountains of California. The icing encounter was entirely in

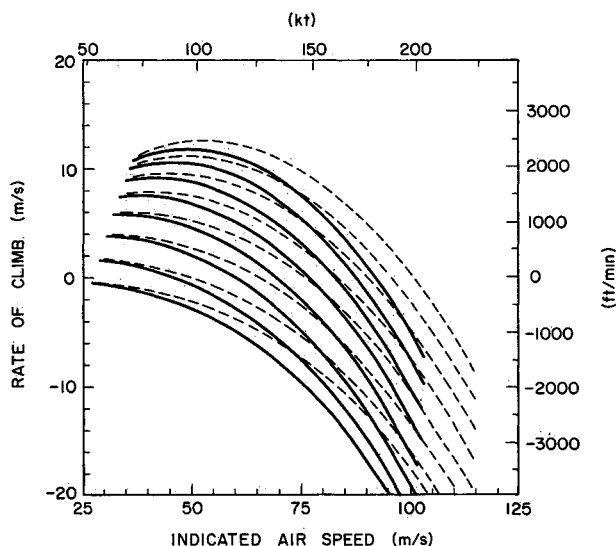


Fig. 5 Rate of climb as a function of airspeed and power setting for the clean airplane (dashed lines) and for the airplane 4.5 h after the start of the March 3, 1980 flight and after ice accumulation (solid lines). The curves correspond to torque settings which start at zero for the lowest curve and increase in increments of 300 ft lb (per engine). The calculations assumed a weight of 10,900 lb, a pressure of 670 mb, and a temperature of -7°C .

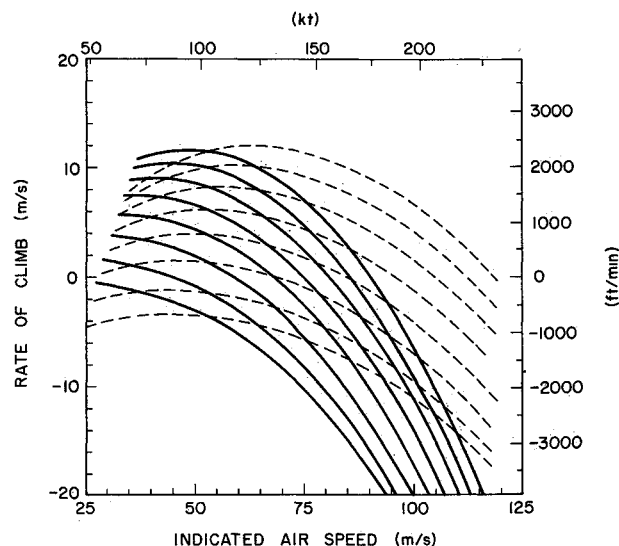


Fig. 6 Rate of climb as a function of airspeed and power setting for the period 2130-2230Z on July 5, 1978 (solid lines), compared to the performance of the clean airplane (dashed lines). The curves correspond to torque settings from 0 to 2100 ft lb in 300 lb increments from bottom to top.

the temperature range warmer than -10°C . The liquid water content was relatively low, about 0.203 g/m^3 when averaged over 17.4 n mi , and D_v was $14.18\text{ }\mu\text{m}$. In 1.5 h , the potential ice accumulation was 11.1 g/cm^2 ; this would correspond to an ice thickness of about 14 cm if the ice density were 0.8 g/cm^3 and the collection efficiency were unity. Actual accumulations on unprotected leading edges were 7.10 cm .

After accumulation of the ice, the performance coefficients were determined to be $C_L = 0.266 + 6.66\alpha$ and $C_D = 0.054$. Figure 5 shows the performance deduced from these coefficients, along with the performance curves obtained from a segment of the flight at the same altitude but before icing occurred. The primary influence of the ice was to increase the drag by about 50% , while the effect on lift was minor.

Figure 6 shows the performance curves determined after an icing encounter on July 5, 1978. This flight encountered a potential accumulation of 19.1 g/cm^2 , the highest in our data set. During this flight, through cumulus clouds in Montana, average liquid water contents exceeded both the intermittent and the continuous maximum criteria of Appendix C. The flight altitude was near $18,000\text{ ft}$ where the temperature was approximately 12°C . During the 2.5 h period of most intense icing, the average liquid water content was 0.23 g/m^3 , and maximum values exceeded 2.5 g/m^3 . The volume median diameter was $17.6\text{ }\mu\text{m}$.

In this case, the performance reduction was minor and there was little degradation in performance after the first 30 min of the 3-h icing encounter. The pneumatic boots (which were used routinely during this and all icing flights) effectively prevented ice from accumulating. As in the March 3, 1980 case, the greatest effect of icing was apparent at high airspeed because the primary effect was to increase the drag of the airframe while causing little change in the coefficient of lift. Figure 6 shows that, even in this case of icing beyond the limits of Appendix C, the airplane retained substantial climb ability.

The above arguments suggest that this airplane has ample reserve power to fly in icing conditions such as those characterized by Appendix C, and this is verified by comfortable flight in most of the icing regions encountered during these research flights. However, in spite of this apparent safety margin, there have been two icing encounters which warranted evasive action.

Potentially Hazardous Icing Encounters

The two icing encounters with the greatest effects on performance (Feb 26, 1982 and Jan 18, 1983) were discussed by Sand et al.¹ Both occurred upwind of the Sierra Nevada Mountains of California. In both cases, the rate of climb of the airplane decreased to 7.9 m/s below that predicted for the clean airframe, and the reduction occurred during icing encounters lasting less than 20 min . The potential accumulations from these cases were only about 3 g/cm^2 , and the ice observed from the cockpit was not commensurate with the effect on performance. When averaged over the continuous maximum distance of Appendix C, the liquid water content was about 0.2025 g/m^3 and D_v was only about $18\text{ }\mu\text{m}$. Over the intermittent maximum distance, the average liquid water content was $<0.3\text{ g/m}^3$. Thus, in terms of the parameters used in Appendix C, these cases appear to be modest icing encounters with the same characteristics that caused no problems during many other flights. Yet, in these two cases, the reduction in climb ability was the greatest we have experienced, and caused the pilots to reverse course and fly out of the icing regions.

Figure 7 (from Ref. 1) shows the contributions to the potential accumulation from hydrometers of various sizes for one of the cases (Feb 26, 1982). The spectrum for Jan 18, 1983 is very similar to this one, but both differ markedly from the spectra in other icing encounters (e.g., Fig. 8). There were substantial contributions to the potential accumulation from hydrometeors with diameters of $40\text{--}300\text{ }\mu\text{m}$ in both of these

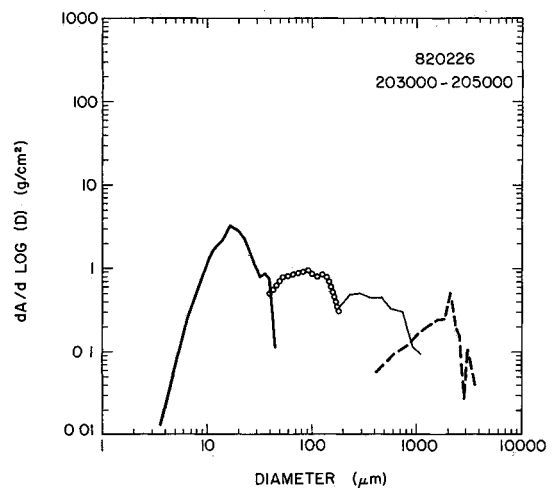


Fig. 7 Contributions of different parts of the hydrometeor spectrum to the potential accumulation (A) of Feb 26, 1982 for the interval 2030-2050Z when the maximum performance degradation occurred. The different curves represent measurements from the different particle measuring probes, the FSSP, 1DC, 2DC, and 2DP in order of increasing size.

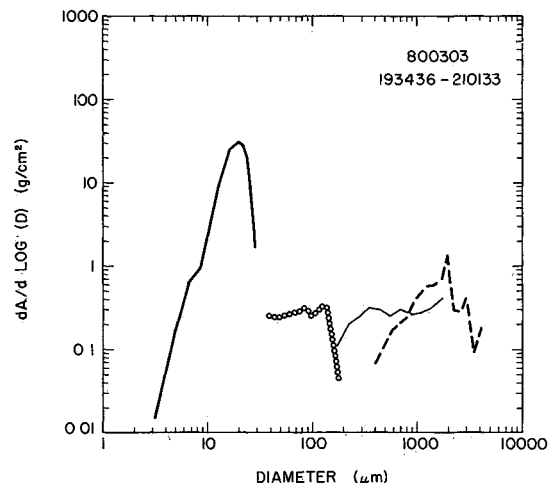


Fig. 8 Contributions of different parts of the hydrometeor spectrum to the potential accumulation (A) of March 3, 1980. All hydrometeors were assumed to be spherical water drops in this calculation although the two-dimensional images indicated that all those larger than $100\text{ }\mu\text{m}$ were ice particles. The plot thus represents an upper limit to the possible contributions from sizes larger than $100\text{ }\mu\text{m}$ because the mass is overestimated by the spherical assumption and the accretion efficiency for ice is likely much less than unity.

cases, and the two dimensional images¹ showed that the hydrometeors less than 0.5 mm in diameter were water drops.

Figure 9 shows the performance characteristics deduced from the period of flight after the icing encounter on Feb 26, 1982, but before the ice was melted from the airframe. The coefficients of lift and drag were found to be $C_L = 0.257 + 3.65\alpha$ and $C_D = 0.049 + 0.075 C_L^2$ just after the icing encounter (leading to Fig. 9), and $C_L = 0.242 + 4.17\alpha$ and $C_D = 0.041 + 0.115 C_L^2$ 5 min later during the porpoising maneuvers. In both cases, the mean coefficient of drag at the prevailing angles of attack was about 0.074 , to be compared with 0.036 for the clean airframe; thus, the coefficient of drag more than doubled during this period of the flight. Although there appears to be a change in the dependence of C_L on angle of attack, in the range of angles of attack from 0.4 deg the net coefficient of lift was nearly the same or slightly higher than for the clean airframe. Thus, the major effect of the ice was to increase the drag substantially. Figure 9 shows that the

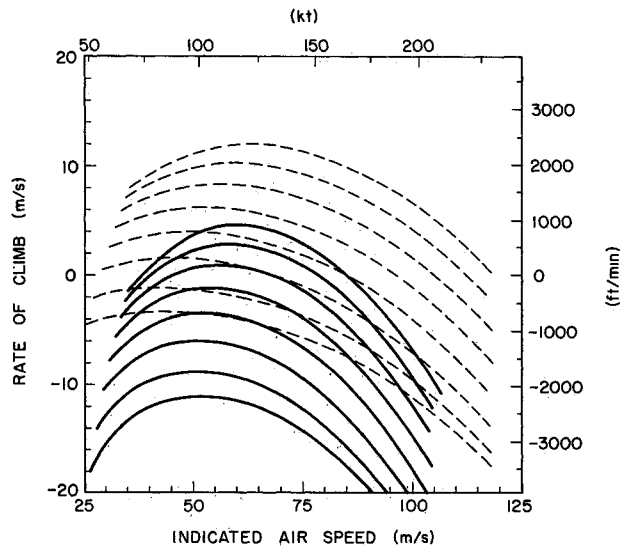


Fig 9 Performance curves for the period 2043 2045Z on Feb 26, 1982 when there was the greatest reduction in performance observed as a result of icing. The solid lines indicate the deduced performance for this interval, and the dashed lines show the performance of the clean airplane without ice. The curves correspond to torque settings from 0 to 2100 ft lb, in increments of 300 ft lb. The assumed prop rotation rate was 1700 rpm.

performance at high airspeed was affected most, but that there was a significant effect on performance at flight speeds from 60 to 100 m/s as well. The maximum indicated airspeed for level flight with a torque setting of 2100 ft lb (near maximum) was only about 85 m/s (~ 165 knots).

During maneuvers to acquire data for the performance evaluation, a pronounced buffet was experienced at indicated airspeeds of 140 knots (72 m/s). This is far above the normal 100-knot (51-m/s) stall speed of this airplane. However, the aircraft was not permitted to stall, therefore, actual stall speed was not determined.

It is interesting to compare the March 3, 1980 and Feb 26, 1982 cases, because the March 3 case appeared on the basis of potential accumulation and median volume diameter to present a more severe icing environment than the Feb 26 case, yet the latter in fact led to much greater degradation in performance. The average liquid water contents and median volume diameters were similar in both cases, and the supercooled water was encountered at similar temperatures in relatively uniform regions of cloud. Yet the March 3 conditions permitted flight over an extended period, while it was soon necessary to divert from the conditions of Feb 26. The major difference was that supercooled drops of intermediate size (40–300 μm) were present Feb 26, but not on March 3.

The authors surmised in Sand et al.¹ that the reason for the difference in performance was that icing occurred on the unprotected lower surfaces of the wings in the Feb 26 case. Although the volume median diameters were about the same in the two cases, the size distribution extended to large sizes on Feb 26 and those large drops were the ones which could accrete on the lower wing surface.

Some calculations following the procedures of Bowden et al.¹⁵ illustrate the importance of large droplets. Although data for the Super King Air airfoil were not available in that report, several other airfoils were discussed. Figure 10 shows the fraction of the lower surface of an NACA 651 208 airfoil (with 1.8 m chord) on which ice could accrete as a function of droplet size. Still larger drops, such as were present on Feb 26, 1982 and Jan 18 1983, would cover distances even greater than these. These distances are substantially greater than those protected by deicing boots or heated surfaces.

The pronounced effect of these large droplets indicates that the characterization of icing conditions according to the

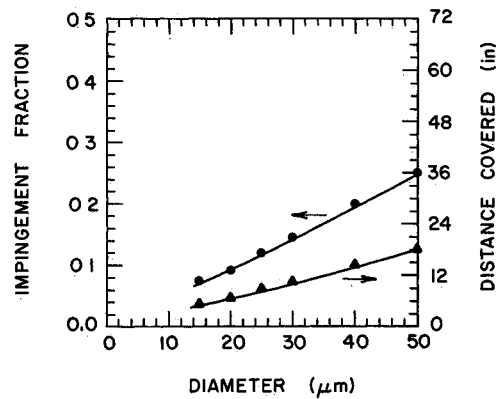


Fig 10 Impingement limits for collision with a NACA 651 208 airfoil at 4 deg angle of attack and for 200 knots true airspeed, 15,000 ft MSL, $+15^\circ\text{F}$, and a chord length of 6 ft. The calculations follow the procedures, and use the data, of Bowden et al.¹⁵

average liquid water content and volume median diameter is incomplete. Although Newton¹⁶ showed that the collection efficiency for droplets of size D_v is often close to the average efficiency of the size spectrum, D_v does not determine the distribution of ice over the accreting surfaces because it conveys no information regarding the breadth of the spectrum about the volume-median size. Contributions from large drops may represent a minor portion of the liquid water content and still have a major influence on performance.

It was found in these two unusual cases, as in the typical cases, that the primary effect of the ice was to increase the drag. The amount of supercooled water in the large drop sizes was not great, but small accretions on the undersides of the wings may have disproportionate effects on performance. The primary effect of such an accretion would be to change the surface roughness. Such an ice surface could have a major effect on drag if it covered a substantial portion of the lower wing surface. This change in surface roughness might also affect the stall characteristics.

There are two important weaknesses in the preceding approach. First, possible effects of icing on propeller efficiency are not included. However, such effects would be associated with small rather than large drops since large drops are likely to be shed from the rapidly moving propellers while small droplets will be collected with high efficiency. The association of this icing encounter with 40–300 μm supercooled drops, the absence of any other anomaly in the microphysical characteristics, and the presence of a buffet at unusually high air speeds all indicate that the effects were not due to changes in propeller efficiency. Second, the two icing encounters being discussed both occurred after installation of the Saunders Failsafe spar strap. This additional structure on the lower wing surface may have worsened the effects of icing there, although the large increase measured in the coefficient of drag and the absence of significant ice accumulations on other unprotected surfaces argue against this spar strap as the primary cause of the performance reduction.

Conclusions

- 1) The liquid water contents and volume median diameters encountered during these research flights generally were consistent with the envelopes of Appendix C, except that no icing regions were encountered in which the volume median diameter was $>30 \mu\text{m}$, while the liquid water content was $>0.2 \text{ g/m}^3$.
- 2) The primary effect of icing was to increase the drag of the airplane by as much as a factor of two. Effects on the coefficients of lift were insignificant.
- 3) Safe flights were conducted in regions where the liquid water contents and volume median diameters spanned the

range of conditions of Appendix C except that the conditions noted in point 1) were not encountered

4) Two unusual cases discussed in the preceding section indicate that rare but potentially hazardous icing conditions occur in which the liquid water content and volume median diameter do not characterize the hazard

Acknowledgments

The U.S. Department of Transportation, FAA Technical Center, Flight Safety Branch, supported research flights to study icing conditions at altitudes below 10,000 ft, and analyses from that contract (DTFA03 81 C 00020) were incorporated into this paper. The conclusions, of course, are those of the authors and do not necessarily reflect the opinions of the sponsors. Support for the acquisition of data used in this research has come from the U.S. Bureau of Reclamation (7-07 83 V0001; wintertime studies by J. Marwitz), the Federal Aviation Administration (DTF01 81 C 00020), the National Science Foundation (via the University of Chicago, courtesy of R. Braham), and the National Oceanic and Atmospheric Administration (via FACE and from A. Auer, PACE)

References

- ¹Sand W. R., Cooper W. A., Politovich, M. K. and Veal D. L. Icing Conditions Encountered by a Research Aircraft accepted for publication, *Journal of Climate and Applied Meteorology* 1984
- ²Federal Aviation Regulations Part 25: Airworthiness Standards Transport Category Airplanes, Federal Aviation Administration, U.S. Government Printing Office Washington D.C. June 1974 (revised edition, May 1982)
- ³Baumgardner D. and Dye, J. E., The 1982 Cloud Particle Measurement Symposium *Bulletin of the American Meteorological Society* Vol 64 April 1983 pp 366 370
- ⁴Cerni, T. A. Determination of the Size and Concentration of Cloud Drops with an FSSP, *Journal of Climate and Applied Meteorology* Vol 22 Aug 1983 pp 1346 1355
- ⁵Neel C. B. and Steinmetz C. P. 'The Calculated and Measured Performance Characteristics of a Heated Wire Liquid Water Content Meter for Measuring Icing Severity' NACA TN 2615, 1952
- ⁶King, W. D., Parkin, D. A., and Handsworth R. J. A Hot Wire Liquid Water Device Having Fully Calculable Response Characteristics *Journal of Applied Meteorology* Vol 17 Dec 1978, pp 1809 1813
- ⁷Strapp, J. W. and Schemenauer R. S. Calibrations of Johnson Williams Liquid Water Content Meters in a High Speed Icing Tunnel *Journal of Applied Meteorology* Vol 21 Jan 1982 pp 98 108
- ⁸Boatman J. F. An Observational Study of the Role of Cloud Top Entrainment in Cumulus Clouds Ph.D. Dissertation University of Wyoming Laramie Wyo., Dec 1981 pp 260 268
- ⁹Rodi A. R. and Spyers Duran, P. Analysis of Time Response of Airborne Temperature Sensors *Journal of Applied Meteorology* Vol. 11, April 1972 pp 554 556
- ¹⁰Lewis W. A Flight Investigation of the Meteorological Conditions Conducive to the Formation of Ice on Airplanes NACA TN 1393, 1947
- ¹¹Lewis W., Kline, D. B., and Steinmetz C. P. A Further Investigation of the Meteorological Conditions Conducive to Aircraft Icing, NACA TN 1424 1947
- ¹²Jeck R. K., 'Icing Characteristics of Low Altitude Supercooled Layer Clouds, FAA RD 80 24 1980
- ¹³Jones A. R. and Lewis, W. Recommended Values of Meteorological Factors to be Considered in the Design of Aircraft Ice Prevention Equipment NACA TN 1855, 1949
- ¹⁴Lenschow D. H. Estimating Updraft Velocity from an Airplane Response *Monthly Weather Review* Vol 104 May 1976 pp 618 627
- ¹⁵Bowden D. T., Gensemer A. E. and Skeen C. A. 'Engineering Summary of Airframe Icing Technical Data' FAA Tech Rept AD 608 865 1964
- ¹⁶Newton D. W. An Integrated Approach to the Problem of Aircraft Icing *Journal of Aircraft* Vol 15 1978 pp 374 380

From the AIAA Progress in Astronautics and Aeronautics Series . . .

VISCOUS FLOW DRAG REDUCTION—v. 72

Edited by Gary R. Hough Vought Advanced Technology Center

One of the most important goals of modern fluid dynamics is the achievement of high speed flight with the least possible expenditure of fuel. Under today's conditions of high fuel costs, the emphasis on energy conservation and on fuel economy has become especially important in civil air transportation. An important path toward these goals lies in the direction of drag reduction, the theme of this book. Historically, the reduction of drag has been achieved by means of better understanding and better control of the boundary layer, including the separation region and the wake of the body. In recent years it has become apparent that, together with the fluid mechanical approach, it is important to understand the physics of fluids at the smallest dimensions, in fact, at the molecular level. More and more, physicists are joining with fluid dynamicists in the quest for understanding of such phenomena as the origins of turbulence and the nature of fluid surface interaction. In the field of underwater motion, this has led to extensive study of the role of high molecular weight additives in reducing skin friction and in controlling boundary layer transition, with beneficial effects on the drag of submerged bodies. This entire range of topics is covered by the papers in this volume, offering the aerodynamicist and the hydrodynamicist new basic knowledge of the phenomena to be mastered in order to reduce the drag of a vehicle.

456 pp 6×9 illus \$25.00 Mem \$40.00 List

TO ORDER WRITE: Publications Order Dept. AIAA 1633 Broadway New York N.Y. 10019